Supplementary Information (SI) for Physical Chemistry Chemical Physics.

Supplementary Information

Improving the Activity of the Oxygen Evolution Reaction on TiN_4-CoN_4 Embedded Carbon Nanotubes via Boron Atom Doping and Uniaxial Strain

Xing-Chen Ding, [a] Bao-Tong Cong, [a] Wen-Hui Zhao, [a] Zi-Qiang Deng, [a] Long-Hui Li, [a] Shi-Yao Liu, [a] Zhen-Kun Tang, [a,*] Hui Zhang [b,*]

[a] *Key Laboratory of Micro-nano Energy Materials and Application Technologies, University of Hunan Province & College of Physics and Electronics Engineering, Hengyang Normal University, Hengyang 421002, China*

[b] *Normal School, Shenyang University, Shenyang 110044, China*

[*] **Author to whom correspondence should be addressed:** zktang@hynu.edu.cn (Z.-K. Tang), huizhangsy@outlook.com (H. Zhang).

OER overpotential calculation details

The OER process involves the dissociation and adsorption of various oxygen-containing intermediates, constituting a complex multi-step reaction pathway. Typically, the reaction comprises four fundamental steps (as shown in Fig. S7),[1] which are described as:

$$* + H_2O(l) \rightarrow {}^*OH + H^+ + e^- \tag{S1}$$

$${}^*OH \rightarrow {}^*O + H^+ + e^- \tag{S2}$$

$${}^*O + H_2O(l) \rightarrow {}^*OOH + H^+ + e^- \tag{S3}$$

$${}^*OOH \rightarrow * + O_2(g) + H^+ + e^- \tag{S4}$$

Where * denotes the surface-active site, (l) and (g) represent liquid and gas phases, respectively. ${}^*OH$, ${}^*O$, and ${}^*OOH$ represent adsorbed intermediates.[2] The adsorption energy of the adsorbed intermediate can be defined by the following equations:

$$\Delta E_{{}^*OH} = E({}^*OH) - E(*) - \left(E_{H_2O} - 1/2E_{H_2}\right) \tag{S5}$$

$$\Delta E_{{}^*O} = E({}^*O) - E(*) - \left(E_{H_2O} - E_{H_2}\right) \tag{S6}$$

$$\Delta E_{{}^*OOH} = E({}^*OOH) - E(*) - \left(E_{H_2O} - 3/2E_{H_2}\right) \tag{S7}$$

where $E(*)$, $E({}^*OH)$, $E({}^*O)$ and $E({}^*OOH)$ are the total surface energy of pure catalyst base and adsorbed by ${}^*OH$, ${}^*O$, and ${}^*OOH$ groups, respectively. E_{H_2O} and E_{H_2} are the total energies of H_2O and H_2 molecules in the gas phase. The Gibbs free energy change ΔG_i (i=1, 2, 3, 4) for the OER step can be defined as:[3]

$$\Delta G_i = \Delta E + \Delta ZPE - T\Delta S \tag{S8}$$

The term ΔE represents the reaction energy difference between reactants and products. ΔZPE stands for zero-point energy, ΔS is the entropy difference between adsorbed and independent states, and T is the reaction temperature (T= 298.15 K). By calculating the vibrational frequencies of adsorbates on the catalyst, the contribution of ZPE in the free energy expression was determined.[4]

By evaluating the catalytic performance through the potential steps of the Oxygen Evolution Reaction (OER), the overpotential (η_{OER}) was proposed under ideal conditions of U = 0 and the Standard Hydrogen Electrode (SHE),[5] defined as: $\eta_{OER} = \max\left(\Delta G_1, \Delta G_2, \Delta G_3, \Delta G_4\right)/e - 1.23V$, In the equation, η_{OER} represents the overpotential for the oxygen evolution reaction (OER). Generally, a lower η_{OER} indicates higher catalytic activity.

To compare the relative stability of the nine B-doped TiN$_4$-CoN$_4$/CNT structures, the formation energies (E_{f1}) can be defined as:

$$E_{f1} = E_{dope} - \left(E_p - \mu_C + \mu_B\right) \tag{S9}$$

Where E_p and E_{dope} represent the total energies of the pristine and doped TiN_4-CoN_4/CNT, respectively. μ_C and μ_B are the chemical potential of C and B atoms. When the energies of μ_C and μ_B are replaced by the energy of a single atom, the formation energies (E_{f2}) can be defined as:

$$E_{f2} = E_{dope} - \left(E_p - E_{single(C)} + E_{single(B)}\right) \tag{S10}$$

The comparative data for the two energy formation methods are presented in Table SI. The binding energy (E_b) of the doped atom and the supporting substrate is given by the following equation:

$$E_b = E_{dope} - E_{def} - E_{single(B)} \tag{S11}$$

Where E_{dope} and E_{def} represent the total energy of the doped TiN_4-CoN_4/CNT, TiN_4-CoN_4/CNT with C vacancy defects, and the $E_{single(B)}$ represents the energy of a single doped B atom.

OER Performance

To gain a systematic understanding of OER performance on B doped TiN_4-CoN_4/CNT structures with different doping sites, the scaling relationship between ΔG_{*OH} vs. ΔG_{*OOH} for the nine doping sites is plotted in Fig. S4(a), and the resulting relationship can be expressed as: $\Delta G_{*OOH} = 1.04\Delta G_{*OH} + 2.94$($R^2$ = 0.95). The ΔG_{*OH} and ΔG_{*OOH} values at the B8 site are lower than those of other structures. By substituting the equation from the above scaling relation into equation (S8), the Gibbs free energy for each step (ΔG_i) can be established as follows:

$$\Delta G_1 = \Delta G_{*OH} \tag{S12}$$

$$\Delta G_2 = \Delta G_{*O} - \Delta G_{*OH} \tag{S13}$$

$$\Delta G_3 = \Delta G_{*OOH} - \Delta G_{*O} = \left(1.04\Delta G_{*OH} + 2.94\right) - \Delta G_1 - \Delta G_2 \tag{S14}$$

$$\Delta G_4 = 4.92 - \Delta G_{*OOH} = 4.92 - \left(1.04\Delta G_{*OH} + 2.94\right) \tag{S15}$$

Besides, the OER performance of TiN_4-CoN_4/CNT-B8 under uniaxial strain is also considered. The obtained scaling relationship can be expressed as: $\Delta G_{*OOH} = 1.18\Delta G_{*OH} + 2.82$($R^2$ = 0.90), and the Gibbs free energy for each step (ΔG_i) can be established as follows:

$$\Delta G_1 = \Delta G_{*OH} \tag{S16}$$

$$\Delta G_2 = \Delta G_{*O} - \Delta G_{*OH} \tag{S17}$$

$$\Delta G_3 = \Delta G_{*OOH} - \Delta G_{*O} = \left(1.18\Delta G_{*OH} + 2.82\right) - \Delta G_1 - \Delta G_2 \tag{S18}$$

$$\Delta G_4 = 4.92 - \Delta G_{*OOH} = 4.92 - \left(1.18\Delta G_{*OH} + 2.82\right) \tag{S19}$$

Calculating the scaling relationship and the Gibbs free energy for each step is a prerequisite for constructing the corresponding volcano plot.

Uniaxial strain calculation details

Uniaxial strain ranging from -10% to +10% was systematically applied to the c-axis lattice constant of TiN_4-CoN_4/CNT-B8. The pristine lattice constant was defined as c, with strain implementations of ±5% resulting in modified lattice constants of $c \times (1 \pm 0.05)$, respectively.

Uniaxial strain ranging from -10% to +10% was systematically applied to the c-axis lattice constant of TiN_4-CoN_4/CNT-B8. The corresponding bond lengths and OER overpotential of TiN_4-CoN_4/CNT-B8 under uniaxial -10% to +10% strain is listed in Table S2, and S4 respectively. Notably, under a -5% compressive strain, the TiN_4-CoN_4/CNT-B8 structure have best OER catalytic activity within the lowest overpotential of 0.32 V.

Table S1 The formation energy (E_f) and binding energy (E_b) of B doped TiN_4-CoN_4/CNT structures with different B doping sites.

Structure	B1	B2	B3	B4	B5	B6	B7	B8	B9
E_{f1}[eV]	3.40	3.71	4.64	3.49	2.86	3.67	4.64	3.81	3.89
E_{f2}[eV]	1.20	1.51	2.44	1.28	0.66	1.47	2.44	1.61	1.69
E_b[eV]	-8.53	-10.91	-10.38	-10.69	-8.57	-11.35	-10.87	-11.80	-9.94

Table S2 Bond lengths of Co-N and B-N under uniaxial strain.

	-10%	-9%	-8%	-7%	-6%	-5%	-4%
B-N	1.468	1.474	1.469	1.463	1.458	1.455	1.453
Co-N1	1.933	1.895	1.86	1.846	1.841	1.839	1.843
Co-N2	1.835	1.808	1.806	1.804	1.804	1.804	1.808
Co-N3	1.852	1.818	1.804	1.798	1.797	1.796	1.801
Co-N4	1.791	1.776	1.821	1.843	1.853	1.850	1.844
	-3%	-2%	-1%	0%	1%	2%	3%

B-N	1.451	1.450	1.449	1.449	1.448	1.447	1.446
Co-N1	1.847	1.853	1.859	1.868	1.880	1.890	1.900
Co-N2	1.812	1.819	1.826	1.833	1.843	1.851	1.859
Co-N3	1.808	1.814	1.820	1.827	1.835	1.843	1.852
Co-N4	1.842	1.843	1.846	1.850	1.855	1.862	1.870

	4%	5%	6%	7%	8%	9%	10%
B-N	1.445	1.444	1.442	1.441	1.439	1.437	1.435
Co-N1	1.911	1.923	1.935	1.946	1.958	1.971	1.988
Co-N2	1.869	1.877	1.887	1.895	1.905	1.914	1.923
Co-N3	1.862	1.870	1.879	1.887	1.893	1.901	1.910
Co-N4	1.879	1.889	1.899	1.910	1.918	1.928	1.942

Table S3 The Bader charge analysis of three catalysts for the oxygenated intermediate *O.

Catalyst	Co	Ti	B	O
TiN$_4$-CoN$_4$/CNT	-1.220	-1.578	/	0.704
TiN$_4$-CoN$_4$/CNT-B8	-1.229	-1.573	-0.214	0.690
TiN$_4$-CoN$_4$/CNT-B8 under -5% strain	-1.242	-1.566	-0.202	0.703

Table S4 The variation of OER overpotential with uniaxial strain for TiN$_4$-CoN$_4$/CNT-B8.

Strain	**-10%**	**-9%**	**-8%**	**-7%**	**-6%**	**-5%**	**-4%**	**-3%**	**-2%**	**-1%**	**0%**
η (V)	1.65	0.54	0.39	0.36	0.34	0.32	0.33	0.35	0.37	0.40	0.41
Strain	**1%**	**2%**	**3%**	**4%**	**5%**	**6%**	**7%**	**8%**	**9%**	**10%**	**/**
η (V)	0.48	0.52	0.54	0.56	0.57	0.59	0.60	0.60	0.61	0.61	

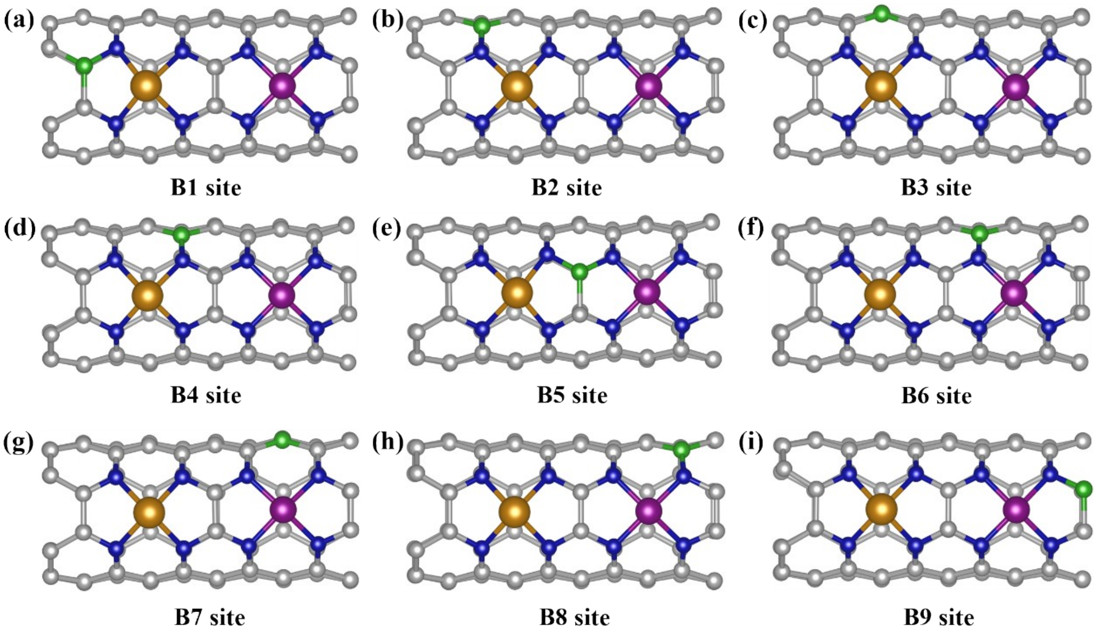

Fig. S1 (a-i) The geometrical configurations of B doped TiN_4-CoN_4/CNT structures with different doping sites. Ti atom are shown in yellow, Co atom in purple, C atoms in grey, N atoms in blue, and B atom in green.

The thermal stability of TiN_4-CoN_4/CNT, TiN_4-CoN_4/CNT-B8, and TiN_4-CoN_4/CNT-B8 under -5% strain in the canonical ensemble (NVT) was investigated through ab-initio molecular dynamics (AIMD) simulations. All three configurations retained structural integrity following 6 ps AIMD simulations at 300 K, demonstrating robust thermal stability under ambient conditions.

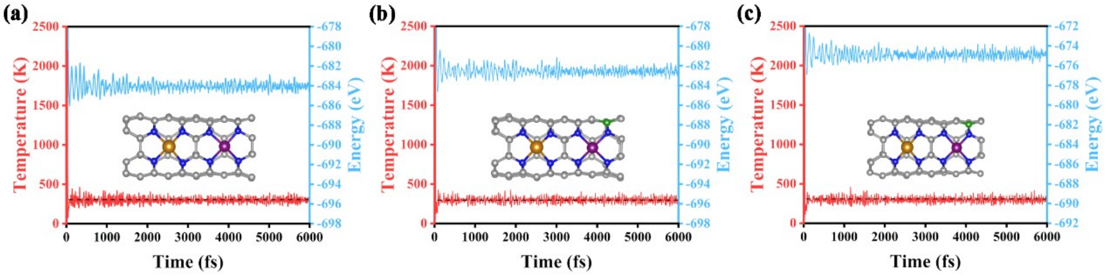

Fig. S2 (a) Energy and temperature variation with AIMD time for TiN_4-CoN_4/CNT at 300 K. (b) Energy and temperature variation with AIMD time for TiN_4-CoN_4/CNT-B8 at 300 K. (c) Energy and temperature variation with AIMD time for the TiN_4-CoN_4/CNT-B8 under -5% strain at 300 K.

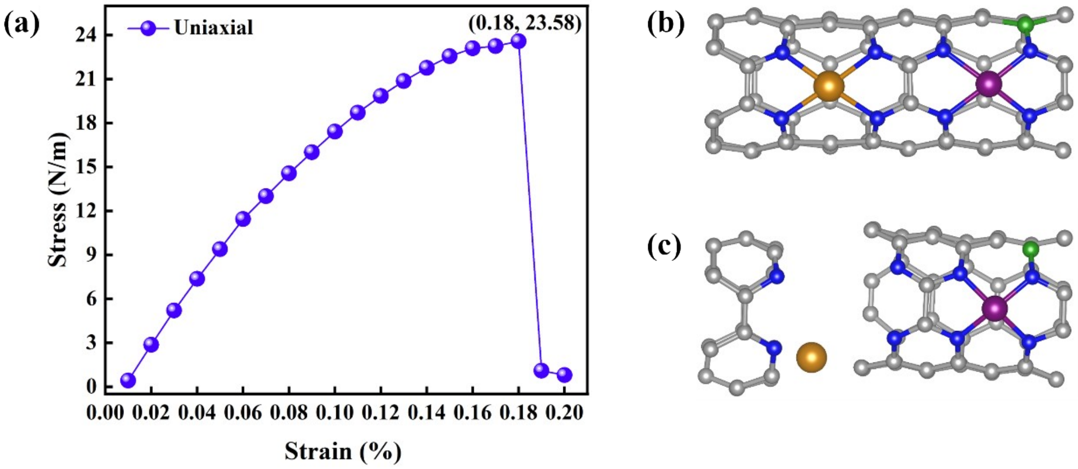

Fig. S3 (a) Uniaxial stress–strain relations of TiN_4-CoN_4/CNT-B8. (b) Optimized structure of TiN_4-CoN_4/CNT-B8 under 18% uniaxial strain. (c) Optimized structure of TiN_4-CoN_4/CNT-B8 under 19% uniaxial strain.

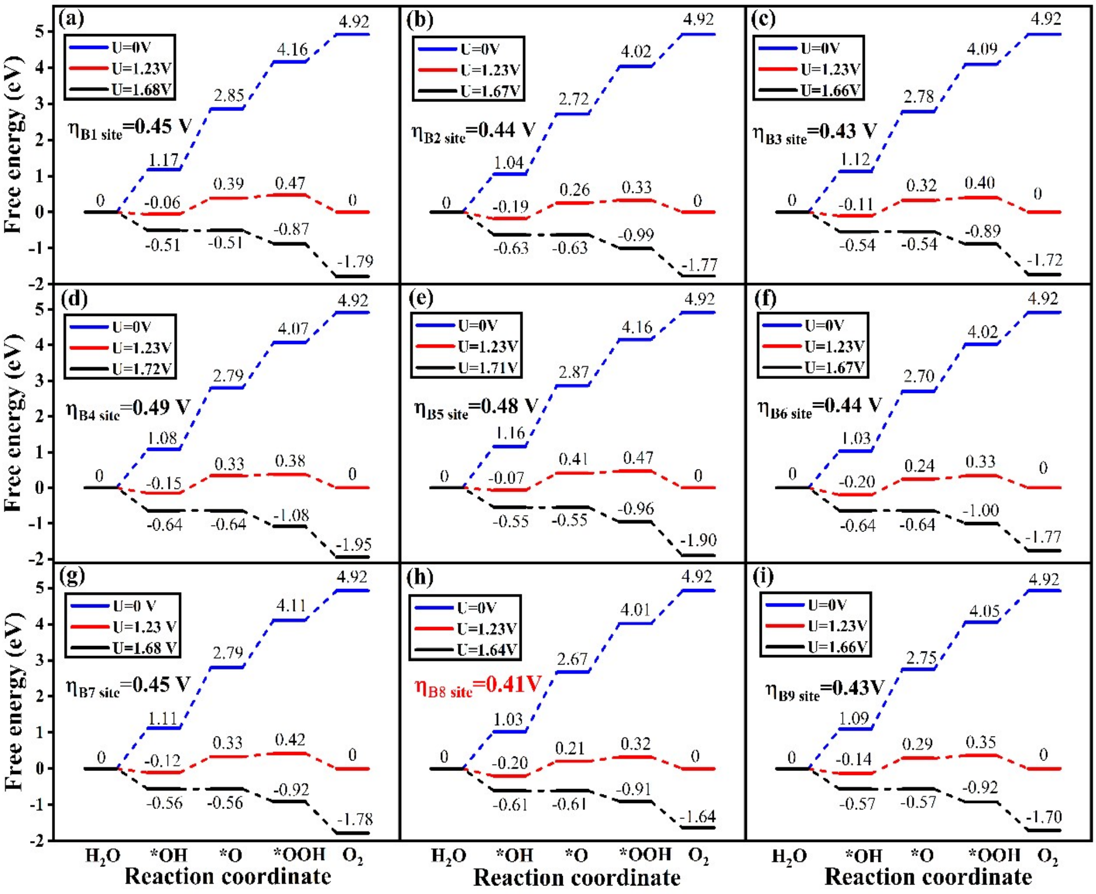

Fig. S4 (a-i) Free energy diagram of CoN_4-TiN_4/CNT with different doping sites.

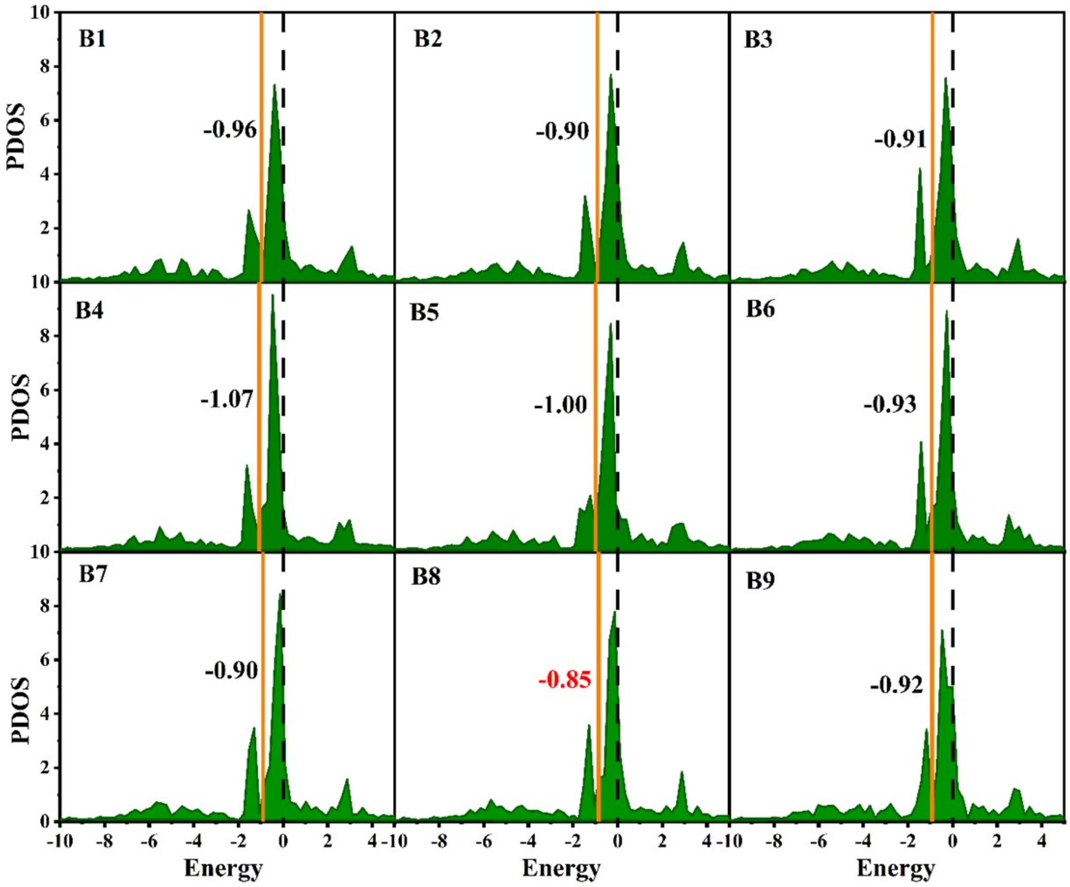

Fig. S5 The partial density of states (PDOS) and d-band centers of B doped TiN_4-CoN_4/CNT structures with different doping sites.

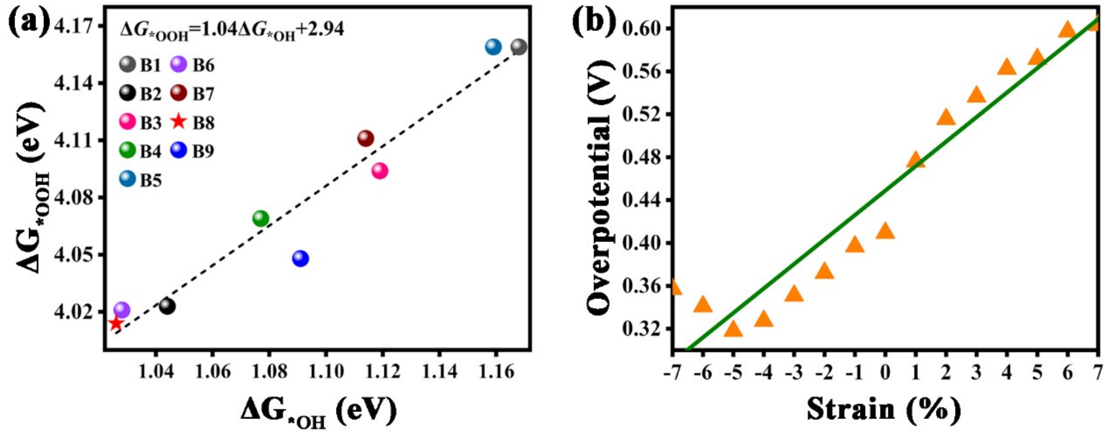

Fig. S6 (a) The scaling relationship between the free energies of *OOH and *OH for the nine B atom doping sites on TiN_4-CoN_4/CNT is depicted by a black dashed line. (b) The variation of OER overpotential with uniaxial strain for TiN_4-CoN_4/CNT-B8. The green line represents a linear fit of the relationship between overpotential and uniaxial strain.

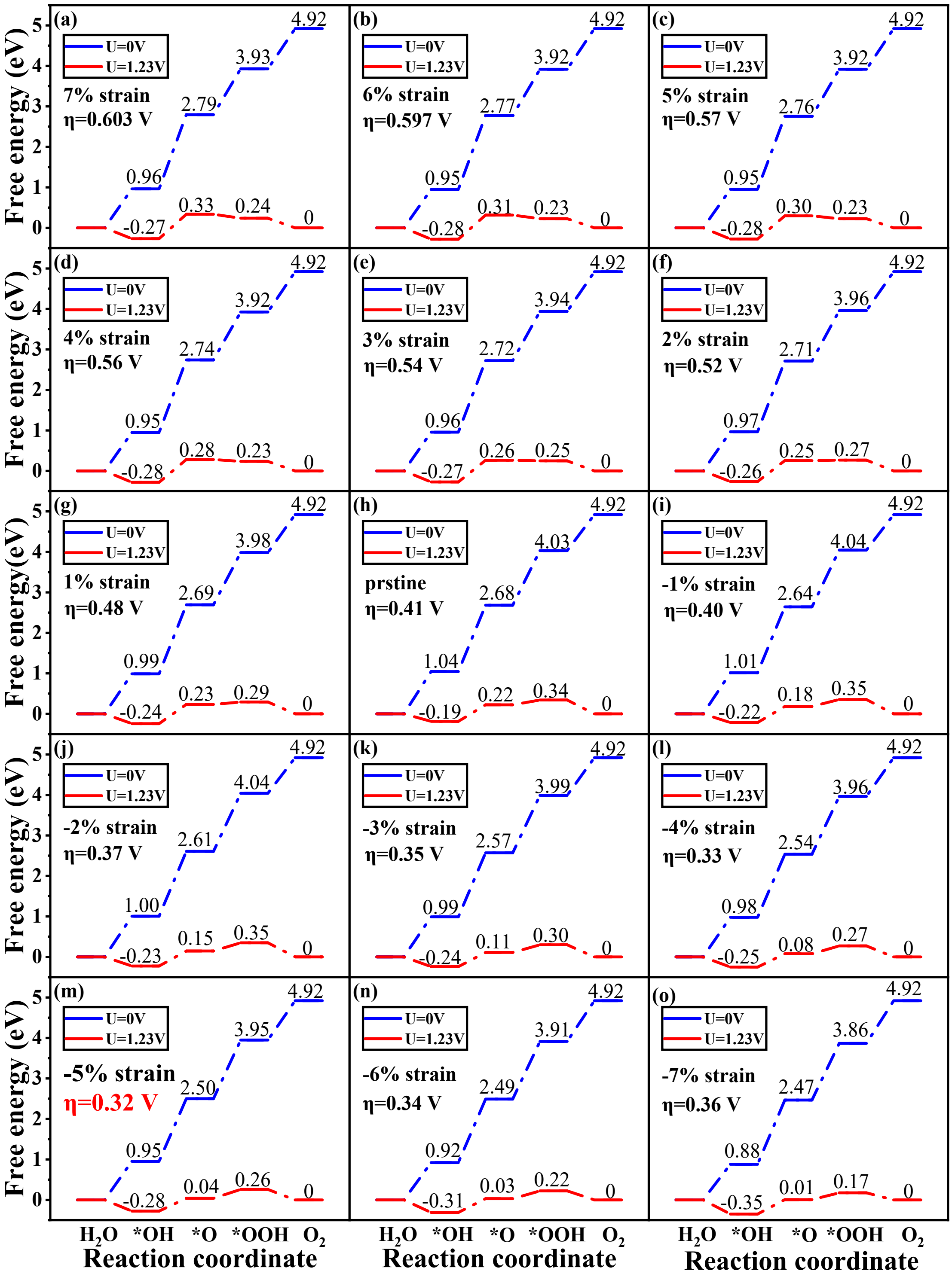

Fig. S7 (a-o) The OER Gibbs free energy diagram of the TiN_4-CoN_4/CNT-B8 under different uniaxial strain levels. The blue line representing U=0 V and the red line represents U=1.23 V.

The free energy profiles of TiN_4-CoN_4/CNT-B8 and TiN_4-CoN_4/CNT-B8 under -5% strain were calculated at a typical potential of 2.0 V, as shown in Fig. S7. The driving forces for each elementary reaction step were additionally presented in Fig. S8 to elucidate catalytic trends. The TiN_4-CoN_4/CNT-B8 catalyst exhibited a minimal energy variation of 0.36 eV during the *OH→*O transition, indicating relatively weak kinetic driving forces in the four-electron OER process. In contrast, the TiN_4-CoN_4/CNT-B8 under -5% strain system demonstrated an enhanced minimal kinetic energy step ~~barrier~~ of 0.45 eV for the *OH→*O conversion, suggesting stronger driving forces along the reaction pathway.

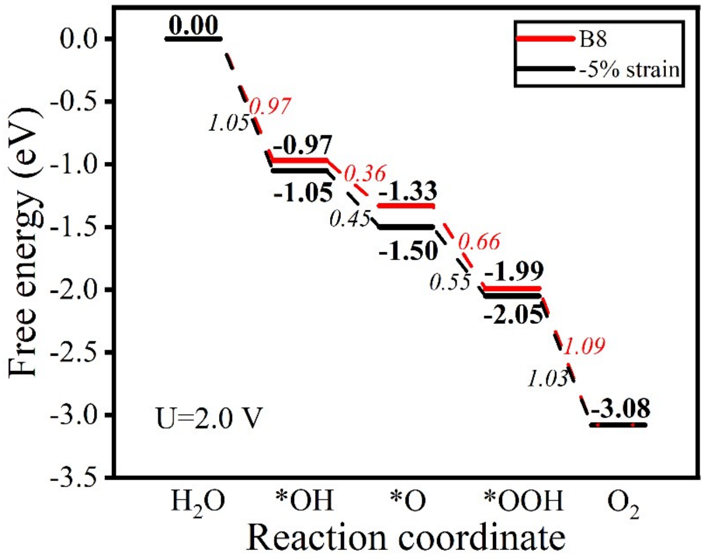

Fig. S8 Detailed free energy profiles of TiN_4-CoN_4/CNT-B8 and TiN_4-CoN_4/CNT-B8 under -5% strain were determined at typical potential of 2.0 V.

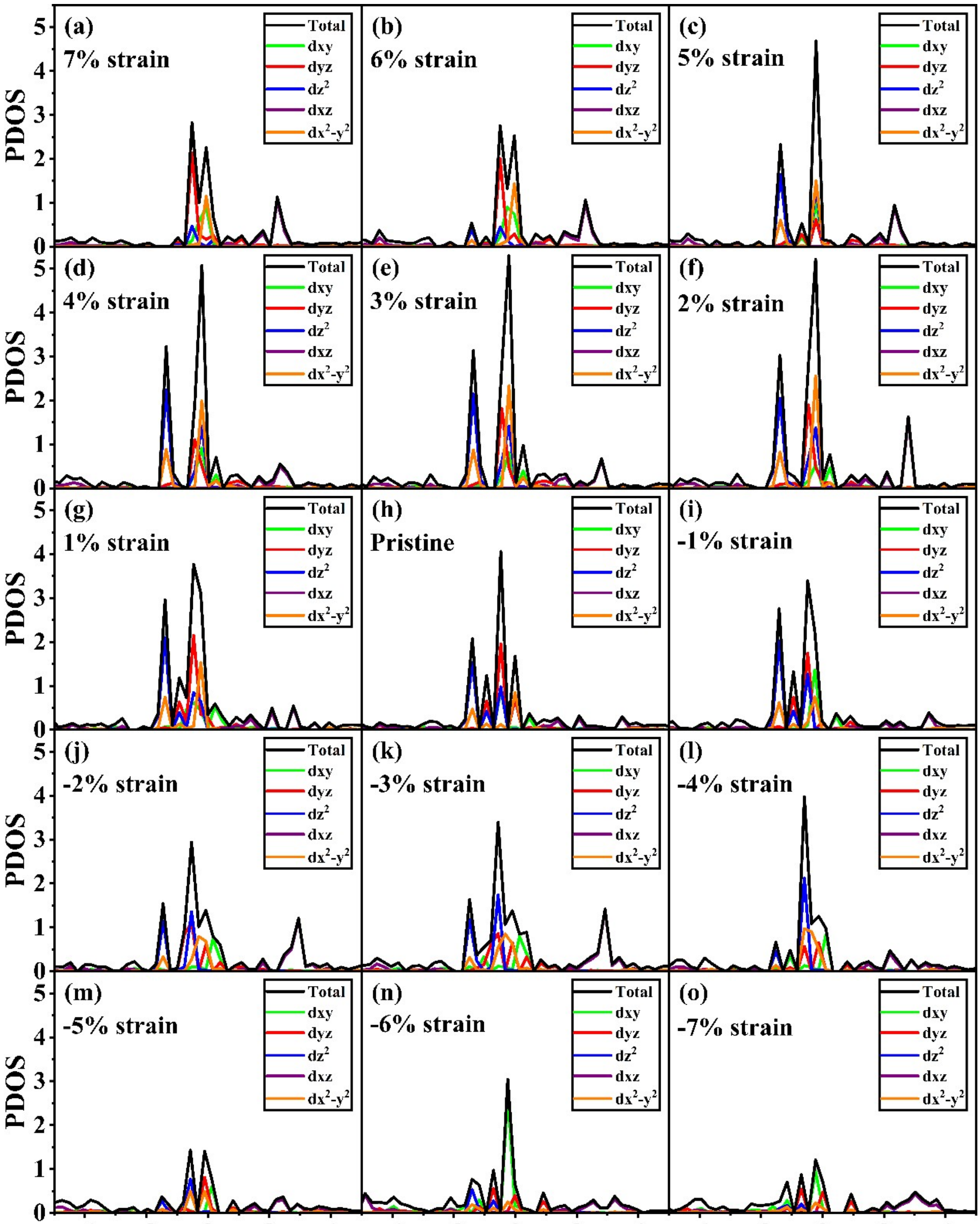

Fig. S9 (a-o) The total density of states (TDOS) and projected density of states (PDOS) of Co-d orbitals in the TiN_4-CoN_4/CNT-B8 structure under different uniaxial strains. The black, red, blue, purple, orange, and green lines represent the TDOS and PDOS of dxy, dyz, dz^2, dxz, and dx^2-y^2, respectively.

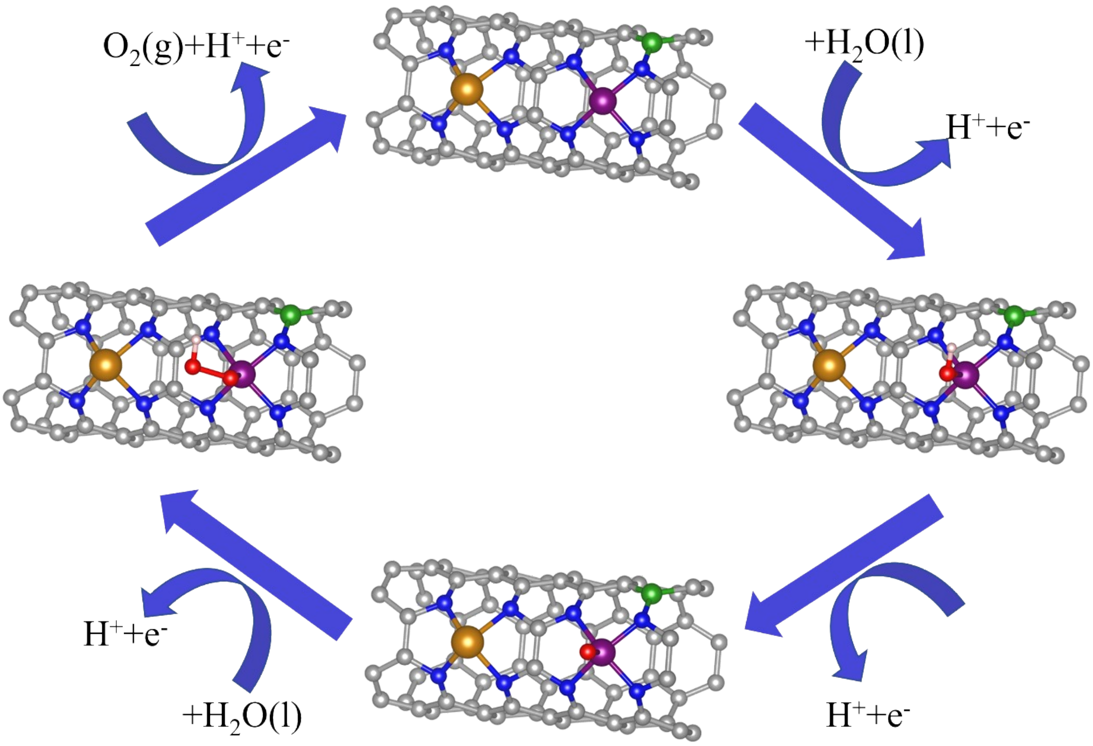

Fig. S10 The OER mechanism diagram of TiN_4-CoN_4/CNT-B8.

Supplementary References

1 Z. W. Seh, J. Kibsgaard, C. F. Dickens, I. Chorkendorff, J. K. Nørskov and T. F. Jaramillo, *Science*, 2017, **355**, eaad4998.

2 W. Yang, Z. Wang, W. Zhang and S. Guo, *Trends in Chemistry*, 2019, **1**, 259–271.

3 J. K. Nørskov, J. Rossmeisl, A. Logadottir, L. Lindqvist, J. R. Kitchin, T. Bligaard and H. Jónsson, *J. Phys. Chem. B*, 2004, **108**, 17886–17892.

4 Á. Valdés, Z.-W. Qu, G.-J. Kroes, J. Rossmeisl and J. K. Nørskov, *J. Phys. Chem. C*, 2008, **112**, 9872–9879.

5 I. C. Man, H. Su, F. Calle-Vallejo, H. A. Hansen, J. I. Martínez, N. G. Inoglu, J. Kitchin, T. F. Jaramillo, J. K. Nørskov and J. Rossmeisl, *ChemCatChem*, 2011, **3**, 1159–1165.